

# Electronic conductance through organic nanowires

S. Jalili<sup>1,2,\*</sup> and H. Rafii-Tabar<sup>2,†</sup><sup>1</sup>*Department of Chemistry, K. N. Toosi University of Technology, P. O. Box 15875-4416, Tehran, Iran*<sup>2</sup>*Computational Physical Sciences Research Laboratory, Department of Nano-Science, Institute for Studies in Theoretical Physics and Mathematics (IPM), P.O. Box 19395-5531, Tehran, Iran*

(Received 16 September 2004; revised manuscript received 1 November 2004; published 8 April 2005)

Quantum-mechanical-based methods are used to obtain the current-voltage ( $I$ - $V$ ) characteristic curves of a molecular nanowire bridging two metallic electrodes. The effect of the molecular electronic structure and mechanism of coupling to the metallic contacts on these curves is investigated for conjugated sulfur-based compounds, oligothiophen. The molecular nanowire is connected to two Au clusters, mimicking the electrodes. The electronic structure of the molecules in the wire was determined using *ab initio*-like calculations. The Hamiltonian matrix elements associated with these molecules were calculated via the density functional theory and the extended Hückel theory methods. The effect of the number of Au contact atoms on the  $I$ - $V$  curves was also investigated using two models; single-atom contact at each electrode and three-atom contact, through the hollow site of the Au(111) plane, at each electrode. We have also investigated the influence of the number of thiophen rings in the wire on the conductance properties. The shapes of the computed  $I$ - $V$  curves are in agreement with the available experimental data.

DOI: 10.1103/PhysRevB.71.165410

PACS number(s): 85.65.+h

## I. INTRODUCTION

A molecular nanowire normally refers to a system composed of a molecule bridging two electron reservoirs. The emerging field of molecular electronics is concerned with constructing information-processing devices by coupling single molecules, with electronic functionalities, together and connecting the resulting nanowire to external electrodes. The design of such a system poses several theoretical, computational, and experimental challenges. Aviram and Ratner<sup>1</sup> were the first to propose sophisticated molecule-based systems analogous to diodes and triodes. Since their proposals, such systems have indeed been synthesized, and some techniques to connect them to external electrodes have been developed. Electronic transport through single, or at most a few, molecules adsorbed on an Au surface was observed with scanning tunneling microscope (STM), where the tip served as a counterelectrode.<sup>2,3</sup> STM can be used not only in the tunneling regime to image adsorbates but also in the contact regime to build few-atom nanoscopic contacts.<sup>4-7</sup> In addition to the STM, mechanically controllable break junctions have also provided powerful tools to study the electronic transport in metallic nanobridges or individual molecules.<sup>8-13</sup>

Connecting a few molecules, or even a single molecule, to conducting electrodes forms the basis of a lively research activity in this field. Examples of nanowires include those constructed from aromatic dithiols,<sup>12</sup> carbon spheres,<sup>14</sup> carbon nanotubes,<sup>15</sup> and alkene thiols.<sup>16</sup>

Molecular wires studied in recent years can be broadly divided into two categories; those based on  $n$ -alkane chains which have a large ( $\sim 6$  eV or greater) band gap separating their highest occupied molecular orbital (HOMO) and their lowest unoccupied molecular orbital (LUMO), and those based on conjugated molecules that have a band gap of  $\sim 2$ – $4$  eV. Members of the first category are relatively insulating and are useful for synthesizing insulating layers, while those in the second category behave very similar to ordinary

semiconductors. Molecules in the latter category possess delocalized  $\pi$  electrons, providing relatively simple systems to study and control, such as conjugated polymers, including polyacetylene, polyaniline, polypyrrole, and polythiophene. Their electrical, optical, and other properties, derived from their delocalized  $\pi$  frameworks, in conjunction with their synthetic and processing advantages as organic polymers, have led to real applications as a new generation of advanced materials. Conjugated oligomers are also interesting materials and have received a great deal of attention. We have chosen oligothiophens due to their multiple potential technological applications. Oligothiophens consist of less than ten thiophen thiol (TT) ring molecules. Many oligothiophens are used in novel electrical or optical devices.<sup>17</sup> They are used in thiophen-based electronic components and devices, such as transistors,<sup>18</sup> electroluminescent devices,<sup>19</sup> photovoltaic cells,<sup>20</sup> energy storage devices,<sup>21</sup> and electrochromic devices.<sup>22</sup> The most important application of these materials is in molecular electronics.

The most common way of connecting conjugated molecules to an electron source/drain is by making a TT-substituted molecule, i.e., a TT molecule in which a hydrogen atom in its end group has been replaced by an S atom, and attaching this to an Au electrode via sulfur-gold (S-Au) binding. In computational modeling of molecular nanowires, the main task has been to provide insight into how the molecule-to-metal electronic coupling and the geometry of the metal contacts affect the flow of current through the wire.

In this paper, we report on first-principles-like calculation of the  $I$ - $V$  characteristic curves of a molecular nanowire composed of a number of TT molecules (rings), as shown schematically in Fig. 1. Furthermore, we have also computed the density of states (DOS) and the transmission function of the nanowire and the electrodes, and have investigated the effect of the contact geometry and the number of TT mol-

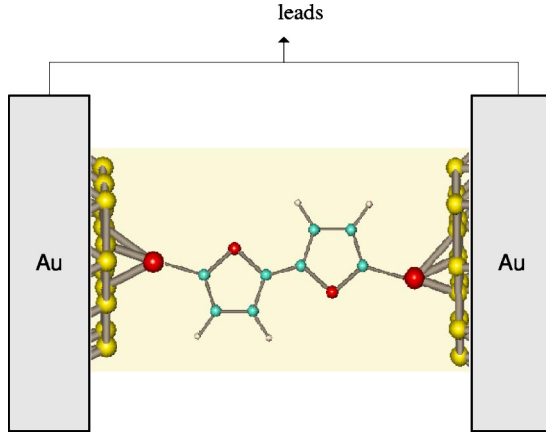


FIG. 1. Schematic illustration of a molecular nanobridge, composed of a conjugated molecule (2TT) chemisorbed onto Au electrodes via the thiol terminal group. The electrodes and the central cluster are shown.

ecules on these properties, as well as on the  $I$ - $V$  curves. The voltage drop due to molecular contact with the electrodes has also been computed, employing the electrostatic potential differences in the presence and absence of an electric field.

The paper is organized as follows. In Sec. II we present the essential computational techniques employed to obtain the conductance properties. Section III provides the computation of the electronic structure of a 2TT system as an example of an oligothiophen. Sections IV and V present the numerical results, together with the concluding remarks.

## II. DETAILS OF THE COMPUTATIONAL TECHNIQUES

### A. General consideration

It is known that conjugated molecules are conductive when connected to metallic leads. However, their electrical resistance is large, so that they cannot be simply used in electronic devices. For this purpose, their resistance should be lowered. A crude expression to calculate the resistance of a molecule is given by<sup>23</sup>

$$R \sim (12.91 \text{ k}\Omega) \exp[0.7245 \sqrt{E_g(\text{eV})L(\text{\AA})}], \quad (1)$$

where the  $L$  is the length of the molecule,  $E_g$  is the band gap energy, and  $12.91 \text{ k}\Omega$  is the quantum of resistance. It should be emphasized that the value of this quantum does not simply refer to the resistance of a molecule, but rather to its as-measured resistance, i.e., when it is attached to two electrodes. The internal resistance of a molecule has, as yet, not been measured. From Eq. (1), we can obtain the approximate value of the resistance of a 2TT system, and this turns out to be

$$R_{(2TT)} \sim 3.385 \text{ M}\Omega, \quad (2)$$

which is quite considerable. However, this value is still in the range for molecules that can be considered as suitable for use in electronic devices.<sup>23</sup>

To compute the current through an organic molecule bridging two metallic electrodes, a rather simple model has

been proposed.<sup>24,25</sup> In this model, shown in Fig. 1, the wire is attached to two atomic clusters representing parts of the two metallic leads, which are themselves modeled as two perfect semi-infinite crystals of the corresponding metal. The molecules together with the two atomic clusters at the ends form a cluster-molecule-cluster (CMC) system, and this system will be referred to as the central cluster. The electronic structure of this central cluster must be resolved in detail since the conductance is mainly determined by the narrowest part of the whole system.<sup>26</sup> We do this via the application of the DFT method.

Consequently, the overall Hamiltonian of the nanobridge is decomposed into

$$\hat{H} = \hat{H}_L + \hat{H}_R + \hat{H}_C + \hat{V}, \quad (3)$$

where  $\hat{H}_C$  describes the CMC, in the absence of the leads, and for this reason we refer to our method as first-principles-like,  $\hat{H}_{L,R}$  describe the left and right leads (electrodes), respectively, and  $\hat{V}$  provides the coupling between the leads and the central cluster, given by<sup>26</sup>

$$\hat{V} = \sum_{ij} v_{ij} (\hat{d}_i^\dagger \hat{c}_j^\dagger + \text{H.c.}), \quad (4)$$

where  $v_{ij}$  are the hopping matrix elements describing the connection between the molecular orbitals of the central cluster  $\hat{c}_j^\dagger$  and the lead orbitals  $\hat{d}_i^\dagger$  and are obtained by reexpressing the molecular orbitals of the central cluster via a Löwdin transformation<sup>27</sup> in terms of atomlike orbitals.

In our implementation of this model, our central cluster consists of the wire and two Au clusters, each composed of 12 Au atoms, at both ends. We have considered two cases: one, the wire coupled, via the S atom, to a single Au atom, and two, the wire coupled to two groups of three Au atoms. Single-atom contacts of a different sort also arise in mechanically controllable break junctions (MCBJs) in which a notched wire is made to break at the notch, resulting in two clean rough fracture surfaces. The surfaces are then brought back into contact, resulting in a point contact due to the roughness of the surfaces. The conductance through this point is then determined.<sup>28</sup>

The current, for a constant bias voltage  $V$  between the metallic leads, is given by the Landauer expression,<sup>29</sup> since the Hamiltonian in Eq. (3) does not contain inelastic scatterings<sup>26</sup>

$$I = \frac{2e}{h} \int_{-\infty}^{\infty} d\epsilon \text{Tr}\{\hat{t}\hat{t}^\dagger\} [f(\epsilon - eV/2) - f(\epsilon + eV/2)], \quad (5)$$

where  $f$  is the Fermi function and  $\hat{t}$  is the energy- and voltage-dependent transmission matrix given by<sup>26</sup>

$$\hat{t}(\epsilon, V) = 2\hat{\Gamma}_L^{1/2}(\epsilon - eV/2)\hat{G}_C^r(\epsilon, V)\hat{\Gamma}_R^{1/2}(\epsilon + eV/2) \quad (6)$$

and the scattering-rate matrices  $\hat{\Gamma}_{L,R}$  are given by

$$\hat{\Gamma}_{L,R} = \text{Im}(\hat{\Sigma}_{L,R}), \quad (7)$$

in which the  $\hat{\Sigma}_{L,R}$  represent the self-energies, containing the information on the electronic structure of the leads and their

coupling to the central cluster. These can be expressed as

$$\hat{\Sigma}_{L,R}(\epsilon) = \hat{v}_{CL,R} g_{L,R}(\epsilon) \hat{v}_{L,R,C}, \quad (8)$$

with  $\hat{v}$  being the hopping matrix which describes the connection between the central cluster and the leads and  $g_{L,R}$  are the Green's functions of the uncoupled leads, i.e., the semi-infinite crystals. We calculated the self-energies of the contact-molecule coupling using the geometry of the contact-molecule connection. The off-diagonal block of  $ES-F$  matrix gives the coupling matrix, where  $S$  and  $F$  are, respectively, the overlap and the Fock matrices, and  $E$  is the energy. The  $S$  and  $F$  matrices were obtained from the GAUSSIAN 98 software. It is evident that the contributions of the left and right leads are taken into account via  $\hat{\Sigma}_L$  and  $\hat{\Sigma}_R$ . A question about the self-energies of the left and right leads that may arise is the reflections at the lead-gold cluster interfaces. It is believed that using the self energies approximation for gold contacts is justified because of two reasons: (1) for bulk gold it is known that around the Fermi energy the local density of states is approximately independent of energy<sup>31</sup> and (2) the transport properties of the molecule are determined by the molecular levels near the Fermi level and the core levels contribute to the total number of electrons by remaining full in the bias range of interest.<sup>32</sup>

To include the scattering process, another self-energy matrix, represented by  $\hat{\Sigma}_p$ ,<sup>33</sup> which reflects the broadening of the energy levels due to coupling to molecular vibrations, is necessary. However, since we have focused on coherent or ballistic transport, we have set  $\hat{\Sigma}_p=0$ .<sup>33</sup> This means that we simply calculated the transmission from the  $L$  contact to the  $R$  contact obtaining a ballistic transport. Consequently, the current in our model is higher than when the scattering process is taken into account. The Green's function of the central cluster is given by

$$\hat{G}_C^r(\epsilon, V) = [\epsilon \hat{1} - \hat{H}_C - \hat{\Sigma}_L(\epsilon - eV/2) - \hat{\Sigma}_R(\epsilon + eV/2)]^{-1}. \quad (9)$$

### B. Density functional based calculations

Quantum chemistry methods can be used to compute the elements of Eq. (9), and one particular approach is to use the Kohn-Sham (KS) Hamiltonian for the central cluster,<sup>30</sup> which in the atomic basis set is represented by<sup>30</sup>

$$\hat{H}_{KS} = \begin{bmatrix} \hat{H}_{LL} & \hat{H}_{LM} & \hat{H}_{LR} \\ \hat{H}_{ML} & \hat{H}_{MM} & \hat{H}_{MR} \\ \hat{H}_{RL} & \hat{H}_{RM} & \hat{H}_{RR} \end{bmatrix}, \quad (10)$$

where  $\hat{H}_{MM}$  represents the matrix elements of the central cluster, 2TT molecule plus two Au clusters, and is assigned to  $\hat{H}_C$  in Eqs. (4) and (9), and  $\hat{H}_{(L,R)M}$  and  $\hat{H}_{M(L,R)}$  are assigned to  $\hat{v}_{CL,R}$  and  $\hat{v}_{L,R,C}$ , respectively, in Eq. (8). These coupling matrices should hypothetically represent the coupling to a geometrically and electronically perfect continuum, but in real situations, such as in a break junction experiment, the molecule is connected through a nanoscopic

tip. Previous *ab initio* studies<sup>30</sup> had shown that the tip atoms tended to arrange themselves in planar structures that included the S atom, as shown in Fig. 1. Then to adapt this procedure to the real conditions, a coupling factor is used as a fitting parameter, affecting the coupling matrix elements  $\hat{H}_{(L,R)M}$  and  $\hat{H}_{M(L,R)}$  and the corresponding elements in the overlap matrix  $S_{ij}$ . A coupling factor of 0.5 was used in those studies. This number is adopted mainly on intuitive geometrical grounds, indicating that the central cluster ends up in a planar shape whose volume is about 50% of what it would be if the ideal continuum were able to hypothetically connect to the molecule. This means that half of the continuum is in direct contact with the central cluster.<sup>30,33</sup> We also employed the same procedure. The  $g_{L,R}$  for Au can be approximated by diagonal matrices with each element proportional to the local DOS of the Au atoms,<sup>33</sup> and were obtained from a theoretical estimation based on the use of tight-binding approximation.<sup>31</sup>

We have used the self-energies in Eq. (9) because the 2TT+Au system does not include the infinite gold contacts, which effectively turn the isolated molecule into an open system. This formulation is one of the standard procedures to study the current through organic molecules connected to metallic leads.

For the description of the Au reservoirs (leads), a basis with the atomlike  $5d$ ,  $6s$ ,  $6p$  orbitals, and for the central cluster the LANL2DZ basis for all atoms<sup>34–36</sup> were used. The DFT-based calculations were performed using the B3LYP method<sup>37,38</sup> via the GAUSSIAN 98 software.<sup>39</sup>

The 2TT system in the nanowire has four H atoms, eight C atoms, and four S atoms. In our calculations we included the  $1s$  orbital of the hydrogen, the  $2s2p$  orbitals of the carbon, and the  $3s3p3d$  orbitals of the sulfur. The matrices  $H$  and  $S$  were computed via the DFT method. For each Au atom we included nine orbitals  $5d6s6p$  and the hopping matrix (or coupling matrix) for each atom was obtained from DFT-based calculations of the central cluster.

It should be emphasized that different approaches can be used, and indeed have been used, for computing the Hamiltonian matrix. These approaches can be listed in two categories, i.e., the *ab initio* and semiempirical methods. In the *ab initio* approach, Hartree-Fock (HF) or DFT methods can be used to compute the electron-electron interactions. In other words, in these methods the correct Hamiltonian of the system is used without including any experimental data other than the values of the fundamental physical constants. The *ab initio* methods are, however, time consuming since they involve the evaluation of the two-electron integrals. Semiempirical molecular quantum-mechanical methods use a Hamiltonian simpler than the correct molecular Hamiltonian. In these methods, some parameters are used whose values are adjusted to fit the experimental data or the results of *ab initio* calculations. Therefore, in these methods, the matrix elements are computed on the basis of rules obtained from a combination of theory and experimental observations.

### C. Extended Hückel theory (EHT) method

A more general and simple method is the EHT which uses all the valence orbitals of the atoms as the basis functions,

e.g., sulfur requires two  $2s$  and four  $2p$  orbitals as the basis. The atomic orbitals can be approximated by the Slater-type orbitals which allow for an efficient computation of the overlap matrix  $S_{ij} = \langle i | j \rangle$ , where  $i$  and  $j$  refer to the orbitals of the central cluster. In the EHT, the Hamiltonian is described via

$$H_{ii} = -V_i \quad (11)$$

and

$$H_{ij} = \frac{c}{2} S_{ij} (H_{ii} + H_{jj}), \quad i \neq j, \quad (12)$$

where the valence orbital ionization energies  $V_i$  are used to approximate the diagonal elements, and the off-diagonal elements are proportional to the overlap, with the constant usually taken to be  $c=1.75$ . Consequently, the Hamiltonian and the overlap matrices can be obtained using these methods.

In this paper, the geometry of all molecules was optimized using the B3LYP/6-31++G\*\* method.<sup>40,41</sup> The conductance properties of the 5, 5'-bi (thiophen thiol), or 2TT, molecule was obtained using the DFT method to study the effect of the contact geometry. To study the effect of the length of the nanowire on the conductance properties, the nonequilibrium Green's function (NEGF), as well as the EHT, methods were used.<sup>42</sup>

### III. COMPUTATION OF THE ELECTRONIC STRUCTURE OF THE 5, 5'-bi (thiophen thiol) (2TT) MOLECULE

The electronic structure of a 2TT molecule is presented as an example of the oligothiophens considered. This molecule contains two S-H terminal groups which covalently bond to the Au electrodes by removing an H atom from each of the S-H groups. These types of molecules have been widely studied experimentally due to their use in molecular junctions.<sup>43</sup> In the 2TT rings the  $\pi$  electrons are delocalized, and this is the main reason for the electronic conductance. The S atom contains free electrons which participate in the ring resonance. For reliability and control of electrical contacts in a metal-molecule heterojunction, the organic molecules are usually functionalized by thiol groups at one or both ends. However, although the role of the S atom in determining the current has been recognized, it has not been fully understood.

There are many experimental results about Au electrodes connected to organic molecules,<sup>23,33,44,45</sup> and we have used Au electrodes so as to be able to compare our results with the available experimental and theoretical data.

The 2TT molecule is symmetrical with a Cs point group. When it is attached to electrodes, it is important to know the position of the Fermi level of the electrodes vis-a-vis the HOMO-LUMO gap of the bridging molecule. We have calculated the energy levels of a single 2TT via the DFT method. The HOMO and LUMO of the 2TT are both  $\pi$  like, and their gap turns out to be 2.362 eV. The HOMO is located at  $-10.5274$  eV, and the LUMO is located at  $-8.1912$  eV. This gap is in the range for conjugated molecules, and thus the 2TT can be conductive. The Fermi level of the molecule is located at  $-10.527$  eV.

Recent experiments have suggested that the binding to a hollow site is energetically more favorable,<sup>46</sup> while others suggest this to be true for a single-atom connection.<sup>12</sup> Consequently, the geometry of a molecule-metal contact is, as yet, not well understood.

We performed quantum-mechanical based calculations, via B3LYP/LANL2DZ, for the 2TT+Au system. For lighter atoms, both the 6-31++G valence triple- $\zeta$  basis set augmented with polarization functions and the LANL2DZ were used.

The S-C bond in the 2TT+Au system is  $1.787$  Å larger than the corresponding bond in the 2TT which is  $1.733$  Å. Since there is no direct experimental information regarding the geometry of the molecule and its attachment to the leads, the overall geometry of the central cluster was relaxed without additional constraints in the calculations, resulting in the Au atoms protruding out of the molecular plane. In the 2TT+Au system, the HOMO is located at  $-9.623$  eV, and the LUMO at  $-8.341$  eV, and the gap is, therefore,  $1.282$  eV, which is less than the gap for the 2TT, i.e.,  $2.362$  eV. This reduction is due to the substitution of the H atoms with the Au atoms, making the molecule conductive.

### IV. COMPUTATION OF THE CONDUCTANCE PROPERTIES OF A 2TT MOLECULE

Here we report on the calculation of the  $I$ - $V$  curves for a 2TT molecule bridging two Au electrodes. It is believed that a critical factor in determining the resistance of a molecular interconnect is the location of the Fermi energy of the metallic contacts relative to the energy levels of the molecule bridging them.<sup>23</sup> Figure 2 is a schematic representation of the energy levels of the molecule relative to the Fermi levels of the Au contacts. The Fermi level alignment in this figure was located using the total DOS of the extended molecule, molecule plus a few Au atoms. From the plot of energy-number of electrons the Fermi energy can be located so as to yield the correct number of electrons in molecule. This method is succinctly described in Ref. 33. We obtained the value of  $-9.32$  eV, coming in the middle of the HOMO and LUMO levels of the molecule given before.

The location of the coupling of the S atom can be at the hollow site or at a single surface atom.<sup>12,47-50</sup> To understand the effect of contact atoms on conducting properties, we examined these two options. Since the conductance is mainly determined by the narrowest part of the bridge, we considered only the detail of the central cluster. For each option, we assumed that the molecule stood perpendicular to the metal surfaces.

The calculated current-voltage curve, obtained via Eq. (5), is shown in Fig. 3. From this figure it can be observed that the current for the case of single-atom contact is approximately 17% smaller than the corresponding current for the case of hollow-site contact. This is not a large value, but forms an appreciable difference. It seems that if the sulfur atom sits directly on top of an Au atom, the overlap of the sulfur  $p_z$  orbital with the  $s$  orbital of the Au atom tends to zero, and this reduces the current. Usually, theoretically determined values of the current are more than 2, or more,



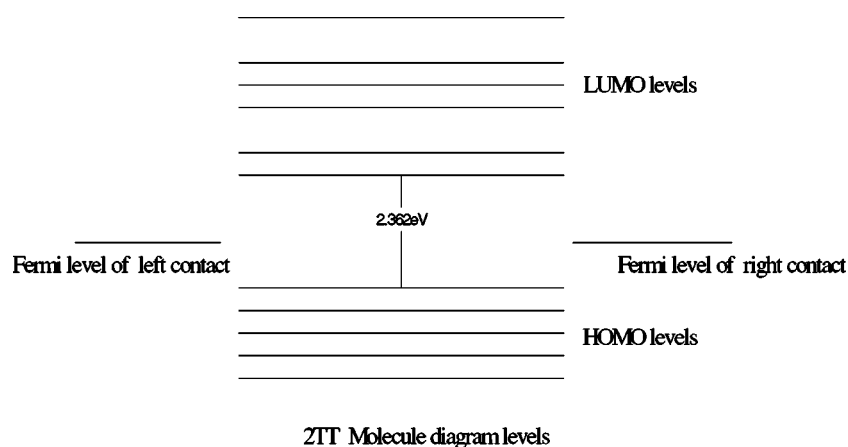


FIG. 2. Schematic diagram for the energy levels of the 2TT molecule, and the relative positions of Fermi level of the Au contacts.

orders of magnitude larger than the measured values.<sup>51</sup> The shape of our computed  $I$ - $V$  curve is similar to the available experimental results, obtained for the oligothiophenes.<sup>43</sup> Other

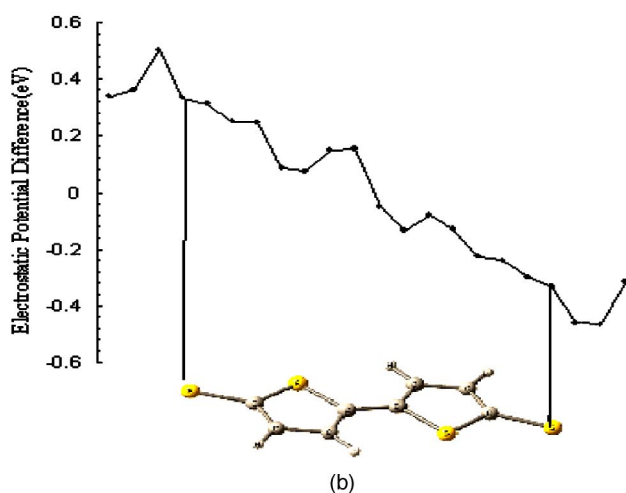
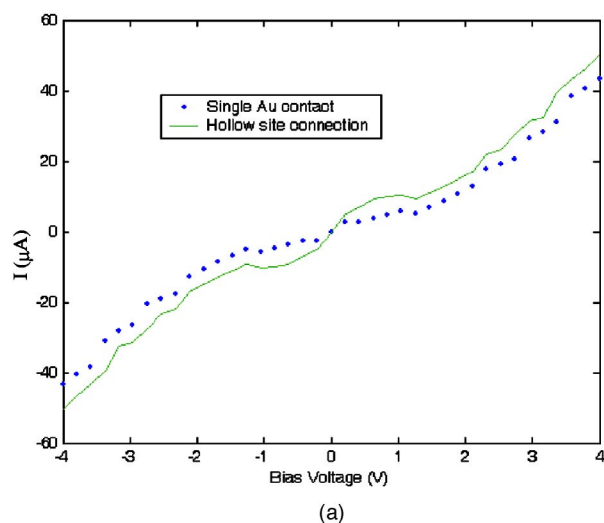


FIG. 3. (a) The  $I$ - $V$  curve for the 2TT molecule. Broken line for single atom contact and solid line for hollow site contact. (b) The voltage drop through the 2TT molecule calculated under 2 V applied voltage bias. The horizontal axis is  $Z$ . (The curves obtained using DFT based calculation.)

computational studies confirm these results.<sup>51</sup> We have also obtained the  $I$ - $V$  characteristic curve for a 4TT system, and this will be reported in the next section. From Fig. 3, it is clear that the computed  $I$ - $V$  curve does not follow an Ohmic pattern. This is a characteristic feature of molecular wires. The 2TT molecule is a symmetric molecule and we expect that its  $I$ - $V$  curve to be also symmetric with respect to  $V=0$ . Figure 3 clearly shows the symmetrical structure of our computed  $I$ - $V$  curve. It should be noted that symmetric molecules can give rise to asymmetric  $I$ - $V$  curves as well. However, as has been demonstrated experimentally,<sup>52,23,26</sup> these are *induced* asymmetries due to, for example, the presence of additional molecules, asymmetrical electrode surfaces, etc.<sup>52</sup> The symmetry of the current with respect to the voltage inversion is important for the behavior of a molecule as a rectifier.<sup>52</sup>

We computed the voltage drop along the 2TT molecule via a simplified DFT-based method in which the difference between the electrostatic potential at finite and zero biases is taken into account.<sup>53</sup> Figure 3 also shows the variations of this voltage drop, showing that it is significant. It has a symmetric structure about the zero point. The voltage drop is important in nonequilibrium devices.<sup>54,55</sup>

## V. COMPUTATION OF CONDUCTANCE PROPERTIES OF OTHER OLIGO THIOPHENS

In this section we investigate the effect of increasing the number of rings in oligothiophen, i.e., the length of the molecular wire, on the  $I$ - $V$  curves and other properties. For this purpose, we employed the NEGF method in conjunction with the EHT method,<sup>56,42</sup> which predicts the one-particle energy levels for a conjugated molecule, to obtain the Hamiltonian matrix for the molecule-contact system in order to compute the  $I$ - $V$  curves and other properties, such as the DOS, the transmission function, and the conductance spectra. We considered five oligothiophens consisting of 1TT, 2TT, 3TT, 4TT, and 5TT rings. In the previous section, the results of the 2TT-based wire were obtained via the DFT method. Here we have recomputed these results, together with those pertinent to the 1TT-, 3TT-, 4TT-, and 5TT-based wires, via the combined NEGF and EHT methods. In all our calculations, we assumed that the oligothiophens were at

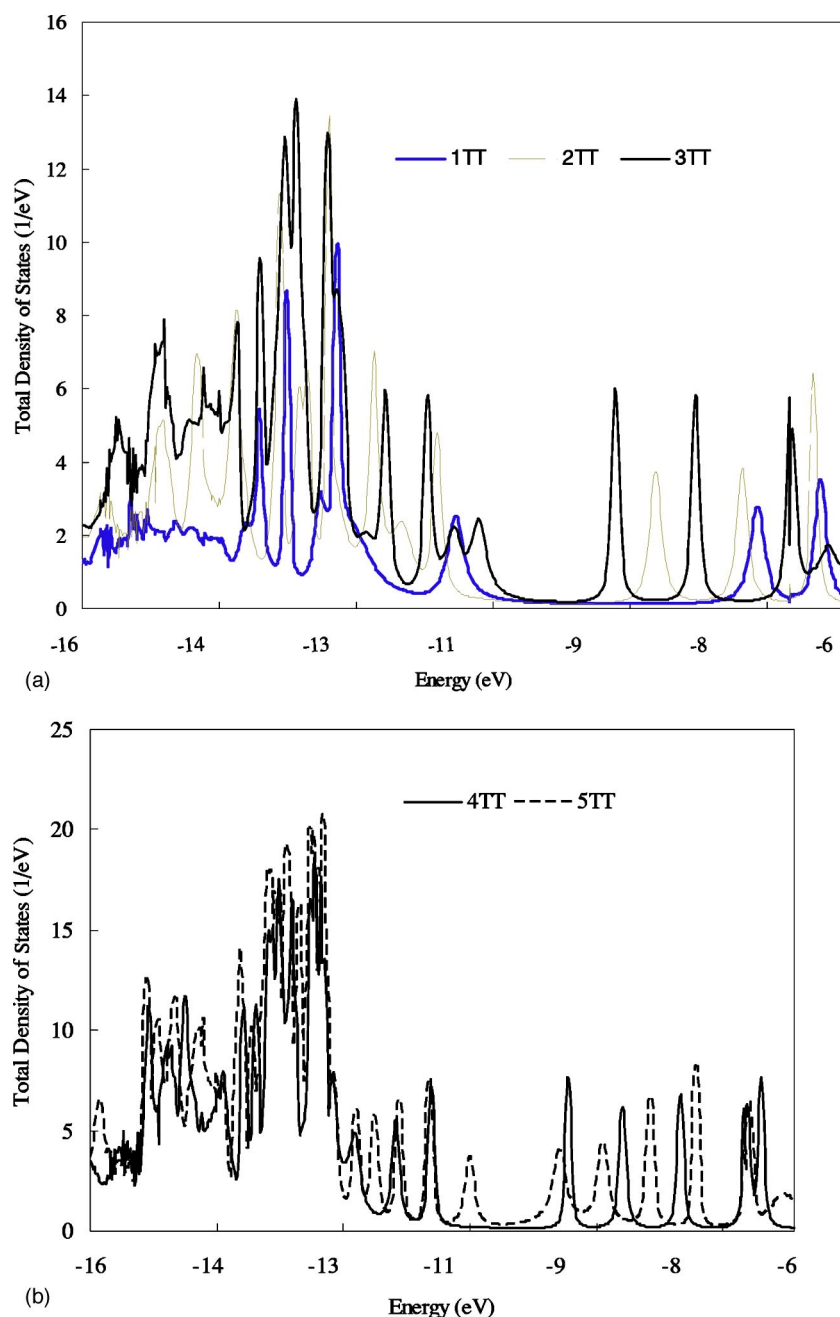


FIG. 4. Calculated density of states (DOS) and transmission function for the 1TT, 2TT, 3TT, 4TT, and 5TT molecules (calculated using EHT method).

tached, via single-atom contact, to the Au(111) surface. Experimental  $I$ - $V$  curves are available for some of these oligothiophenes,<sup>43</sup> and we have been able to compare our results with these.

The structure of all the oligothiophenes were optimized at the B3LYP/6-31++G\*\* level of theory as implemented in GAUSSIAN 98 program.<sup>39</sup> The DOS and transmission diagrams of these systems are shown in Fig. 4. The Fermi energies for these systems lie in their HOMO-LUMO band gaps. The HOMO for all these oligothiophenes becomes broader due to their coupling to the Au contacts, and this broadening enhances the electronic transmission. The  $I$ - $V$  curves pertinent to the five oligothiophene nanowires are shown in Fig. 5. It is important to note that for all the systems the transmission is strongest in the region where the Au states have coupled with the molecular states. In the region where there is a resonance

between the Au orbitals and the HOMO of the oligothiophen, there appear peaks in the transmission graphs. It is interesting to note from Fig. 4(b) that the transmission near the HOMO-LUMO gap in the 1TT-based nanowire is greater than in the other size wires, in contrast to what one might expect.

The LUMO in all the above systems is also coupled with the Au states. But it is clear that the contribution from these to the transmission is smaller than the contribution from HOMOs' combination with the Au states.

The transmission through all these systems resembles closely the DOS for these systems. For the 1TT molecule, this resemblance is stronger. If the 1TT molecule connects to one Au contact stronger than the other Au contact, then the peaks in the DOS diagram should be wide and the transmission peaks should be narrow, which should be the case for

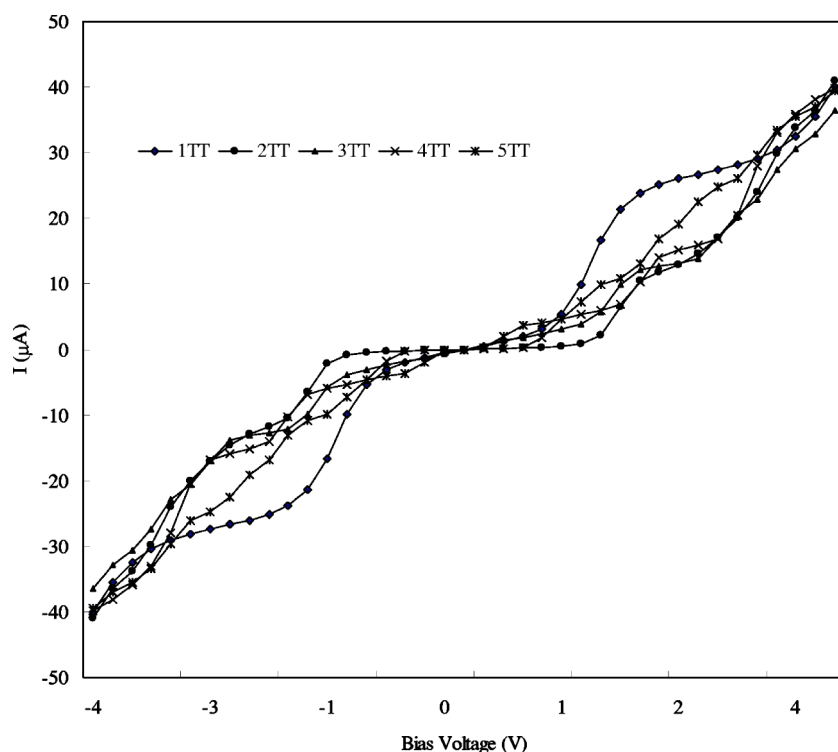


FIG. 5. Calculated  $I$ - $V$  characteristic curves for the molecules in Fig. 5 (calculated using the EHT method). The Fermi energies for 1TT, 2TT, 3TT, 4TT, and 5TT molecules are  $-9.83$ ,  $-8.60$ ,  $-9.12$ ,  $-8.48$ , and  $-9.65$  eV, respectively.

asymmetric wave functions pertinent to the 1TT, 3TT, and 5TT systems. But, we see that the DOS and the transmission diagrams do not show such a behavior, and this implies that the 1TT molecule was connected to both Au contacts strongly. This behavior, i.e., the strong connectivity to both contacts, is also observed for other oligothiophenes. By increasing the system's length, the size of the flat region in the DOS diagrams, which is a measure of the HOMO-LUMO band gap, decreases progressively from the 1TT to the 5TT oligothiophen, as expected for such systems, due to better overlap of the  $p$  orbitals which gives the  $\pi$  orbitals.

Another interesting question that we have explored concerns the effect of the number of sulfur atoms in the wire, which bind strongly to Au leads, on its conductance properties. In the five systems considered in this paper, it seems that the number of S atoms affects the conductance properties. One expects that by increasing the number of  $\pi$  electrons, the system becomes more conductive. The sulfur atoms, however, partially insulate the  $\pi$ -electron states of the molecules, leading to a decrease in their conductivity. Similar results have been obtained for phenyl dithiol.<sup>33</sup>

All the systems considered here show nonlinear behavior in their  $I$ - $V$  curves. The conductance characteristics and the conductance spectra for these systems are shown in Fig. 6. These curves were obtained via a modified version of Hückel-IV method, the details of which can be found elsewhere.<sup>33</sup> An interesting point in Fig. 5 is the region around the zero voltage in the  $I$ - $V$  curves. For the systems with an odd number of TT rings, the current increases smoothly, but for the systems with an even number of TT rings, the current seems to stay constant. The reason could be due to the stronger coupling of the 1TT, 3TT, and 5TT systems to the Au contacts compared with the coupling of the 2TT and 4TT systems. We should emphasize that this result

may not be a universal result and that it may not manifest itself in other molecular wires.

Experimental results are available for the 4TT-based molecular wire.<sup>43</sup> The shape of our calculated  $I$ - $V$  curve for this wire, shown in Fig. 5, is similar to the experimental curve but the magnitude of the computed current is larger than the experimental value. Since we cannot accommodate all of the factors influencing the value of the current, such as the various molecular conformations, the electronic structure of the molecules and the geometry of the molecule-electrode contact, we do not expect the calculated values to be in very good agreement with the experimental values. The aim of this work, and other works such as ours, is to find some clues about the parameters which influence the current through the molecular wires, as such results will help in designing molecule-based electronic devices.

The conductance spectra corresponding to the  $I$ - $V$  curves in Fig. 5 are shown in Fig. 6. We expect that by increasing the number of TT rings in the wire, the HOMO-LUMO gap to become smaller. Figure 6 shows this expected behavior, with the conductance increasing as a result. This increase is due to the resonance tunneling through the molecular states. The peaks in Fig. 6, which were observed at energies corresponding of the molecular energies of the thiophen systems, were due to this resonant tunneling. It is clear that by increasing the number of rings the number of peaks increases because of an increase in the number of the molecular states, and the same applies for the resonant tunneling. The width of the peaks show that the broadening of the molecular levels was due to the Au contacts.

To sum up, we have computed the  $I$ - $V$  characteristics of a set of thiophen thiol (TT)-based nanowires, using first-principles-like methods. We have found that the  $I$ - $V$  curves for all the TT-based systems were non-Ohmic in character.

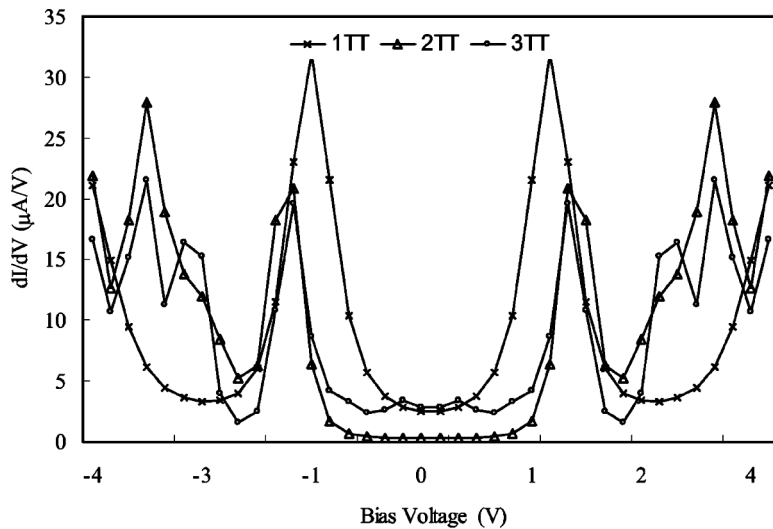
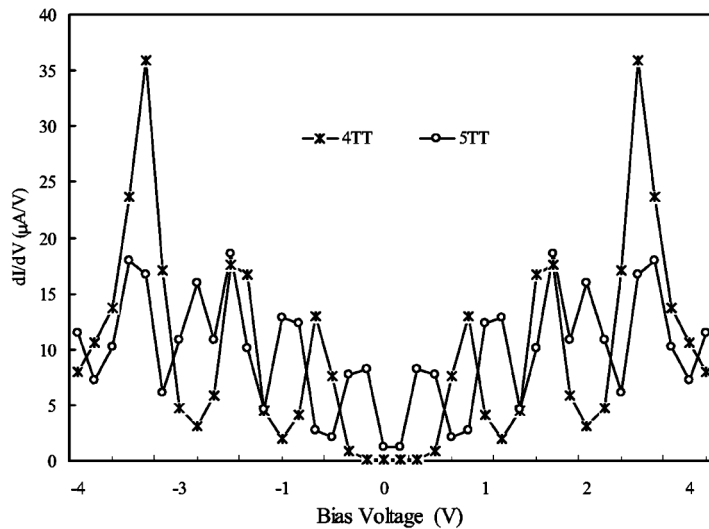


FIG. 6. Conductance in molecules in Fig. 5 as a function of the bias potential applied to the Au contacts (calculated using the EHT method).



We considered two modes of contact between the wire and the Au electrodes; single-atom contact, and contact to the hollow site of the Au(111) plane. It seems that the former contact geometry was more effective for the conduction. The experimental results also show that contacts are indeed more likely to be atomically terminated.<sup>12</sup>

We also found that the length of the molecular wire was an important factor influencing the conductance properties.

Also, the presence of the sulfur atoms critically affected the value of the current.

For future research, it is worthwhile to explore the role of the molecular conformations and the effect of local disorder in the leads, as well as the role of the temperature and pressure. A further useful study can be to test the effect of electron donating and electron withdrawing groups on the rings themselves.

\*Email address: sjalili@nano.ipm.ac.ir

†Email address: rafii-tabar@nano.ipm.ac.ir

<sup>1</sup>A. Aviram and M. A. Ratner, Chem. Phys. Lett. **29**, 277 (1974).

<sup>2</sup>S. Datta, W. Tian, S. Hong, R. Reifenberger, J. I. Henderson, and C. P. Kubiak, Phys. Rev. Lett. **79**, 2530 (1997).

<sup>3</sup>C. Joachim, J. K. Gimzewski, R. R. Schlittler, and C. Chavy, Phys. Rev. Lett. **74**, 2102 (1995).

<sup>4</sup>D. Porath, Y. Levi, M. Tarabiah, and O. Millo, Phys. Rev. B **56**,

9829 (1997).

<sup>5</sup>J. G. Hou, J. Yang<sup>1</sup>, H. Wang, Q. Li, C. Zeng, H. Lin, W. Bing, D. M. Chen, and Q. Zhu, Phys. Rev. Lett. **83**, 3001 (1999).

<sup>6</sup>N. Agrait, J. C. Rodrigo, and S. Vieira, Phys. Rev. B **47**, 12 345 (1993).

<sup>7</sup>J. I. Pascual, J. Méndez, J. Gómez Herrero, A. M. Baró, N. García, and V. T. Binh, Phys. Rev. Lett. **71**, 1852 (1993).

<sup>8</sup>C. J. Muller, J. M. Ruitenbeek, and L. J. Jong, Phys. Rev. Lett.



- 69**, 140 (1992).
- <sup>9</sup>J. M. Krans, J. M. van Ruitenbeek, V. V. Fisun, I. K. Yanson, and L. J. de Jongh, *Nature (London)* **375**, 767 (1995).
  - <sup>10</sup>A. I. Yanson and J. M. Ruitenbeek, *Phys. Rev. Lett.* **79**, 2157 (1997).
  - <sup>11</sup>E. Scheer, N. Agrait, J. C. Cuevas, A. L. Yeyati, B. Ludoph, A. Martin-Rodero, G. R. Bollinger, J. M. van Ruitenbeek, and C. Urbina, *Nature (London)* **394**, 154 (1998).
  - <sup>12</sup>M. A. Reed, C. Zhou, C. J. Muller, T. P. Burgin, and J. M. Tour, *Science* **278**, 252 (1997).
  - <sup>13</sup>H. Park, J. Park, A. K. L. Lim, E. H. Anderson, A. P. Alivisatos, and P. L. McEuen, *Nature (London)* **407**, 57 (2000).
  - <sup>14</sup>C. Joachim, *Phys. Rev. Lett.* **74**, 2102 (1995).
  - <sup>15</sup>S. C. Tans, R. M. Verschueren, and C. Dekker, *Nature (London)* **393**, 49 (1998).
  - <sup>16</sup>R. P. Anders, J. D. Bielefeld, J. I. Henderson, D. B. Janes, V. R. Kolagunta, C. P. Kubiak, W. J. Mahoney, and R. G. Osifchin, *Science* **273**, 1690 (1997).
  - <sup>17</sup>D. Fichou, *J. Mater. Chem.* **10**, 571 (2000).
  - <sup>18</sup>G. Horowitz, *Adv. Mater. (Weinheim, Ger.)* **10**, 365 (1998).
  - <sup>19</sup>T. Noda and Y. Shirota, *J. Am. Chem. Soc.* **120**, 9714 (1998).
  - <sup>20</sup>N. Noma, T. Tsuzuki, and Y. Shirota, *Adv. Mater. (Weinheim, Ger.)* **7**, 647 (1995).
  - <sup>21</sup>T. Yamamoto, M. Zama, and A. Yamamoto, *Chem. Lett.* **1985**, 563.
  - <sup>22</sup>F. Garnier, G. Tourillon, M. Gizard, and J. C. Dubois, *J. Electroanal. Chem. Interfacial Electrochem.* **148**, 299 (1983).
  - <sup>23</sup>C. Kergueris, J. P. Bourgoin, and S. Palacin, *Nanotechnology* **10**, 8 (1999).
  - <sup>24</sup>R. Hofmann and J. Lipscomb, *J. Chem. Phys.* **37**, 2872 (1963).
  - <sup>25</sup>R. Hofmann, *J. Chem. Phys.* **40**, 2747 (1964).
  - <sup>26</sup>J. Heurich, J. C. Cuevas, W. Wenzel, and G. Schn, *Phys. Rev. Lett.* **88**, 256803 (2002).
  - <sup>27</sup>P. O. Löwdin, *J. Chem. Phys.* **18**, 365 (1950).
  - <sup>28</sup>N. Agrait, A. L. Yeyati, and M. van Ruitenbeek, *Phys. Rep.* **377**, 81 (2003).
  - <sup>29</sup>R. Landauer, *IBM J. Res. Dev.* **1**, 223 (1957).
  - <sup>30</sup>P. A. Derosa and J. M. Seminario, *J. Phys. Chem. B* **105**, 471 (2001).
  - <sup>31</sup>D. A. Papaconstatopoulos, *Handbook of the Band Structure of Elemental Solids* (Plenum, New York, 1980).
  - <sup>32</sup>P. S. Damle, A. W. Ghosh, and S. Datta, *Chem. Phys.* **281**, 171 (2002).
  - <sup>33</sup>W. Tian, S. Datta, S. Hong, R. Reifengerger, J. I. Henderson, and C. P. Kubiak, *J. Chem. Phys.* **109**, 2874 (1998).
  - <sup>34</sup>P. J. Hay and W. R. Wadt, *J. Chem. Phys.* **82**, 270 (1985).
  - <sup>35</sup>W. R. Wadt and P. J. Hay, *J. Chem. Phys.* **82**, 284 (1985).
  - <sup>36</sup>P. J. Hay and W. R. Wadt, *J. Chem. Phys.* **82**, 299 (1985).
  - <sup>37</sup>A. D. Beck, *Phys. Rev. A* **38**, 3098 (1988).
  - <sup>38</sup>C. Lee, W. Yang, and R. G. Parr, *Phys. Rev. B* **37**, 785 (1988).
  - <sup>39</sup>M. J. Frisch, G. W. Trucks, H. B. Schlegel, G. E. Scuseria, M. A. Robb, J. R. Cheeseman, V. G. Zakrzewski, J. A. Montgomery, Jr., R. E. Stratmann, J. C. Burant, S. Dapprich, J. M. Millam, A. D. Daniels, K. N. Kudin, M. C. Strain, O. Farkas, J. Tomasi, V. Barone, M. Cossi, R. Cammi, B. Mennucci, C. Pomelli, C. Adamo, S. Clifford, J. Ochterski, G. A. Petersson, P. Y. Ayala, Q. Cui, K. Morokuma, D. K. Malick, A. D. Rabuck, K. Raghavachari, J. B. Foresman, J. Cioslowski, J. V. Ortiz, B. B. Stefanov, G. Liu, A. Liashenko, P. Piskorz, I. Komaromi, R. Gomperts, R. L. Martin, D. J. Fox, T. Keith, M. A. Al-Laham, C. Y. Peng, A. Nanayakkara, C. Gonzalez, M. Challacombe, P. M. W. Gill, B. Johnson, W. Chen, M. W. Wong, J. L. Andres, C. Gonzalez, M. Head-Gordon, E. S. Replogle, and J. A. Pople, *GAUSSIAN 98*, Revision A.6, 1998, Gaussian, Inc., Pittsburgh, PA.
  - <sup>40</sup>R. Ditchfield, W. J. Hehre, and J. A. Pople, *J. Chem. Phys.* **54**, 724 (1971).
  - <sup>41</sup>W. J. Hehre, R. Ditchfield, and J. A. Pople, *J. Chem. Phys.* **56**, 2257 (1972).
  - <sup>42</sup>F. Zahid, M. Paulsson, and S. Datta, *Electrical Conduction Through Molecules*, edited by H. Morkoc (Academic Press, New York, 2003).
  - <sup>43</sup>N. B. Zhitenev, H. Meng, and Z. Bao, *Phys. Rev. Lett.* **88**, 226801 (2002).
  - <sup>44</sup>S. N. Rashkeev, M. D. Ventra, and S. T. Pantelides, *Phys. Rev. B* **66**, 033301 (2002).
  - <sup>45</sup>M. P. Samanta, W. Tian, S. Datta, J. I. Henderson, and C. P. Kubiak, *Phys. Rev. B* **53**, R7626 (1996).
  - <sup>46</sup>L. A. Bumm, J. J. Arnold, M. T. Cygan, T. D. Dunbar, T. P. Burgin, L. Jones II, D. L. Allara, J. M. Tour, and P. S. Weiss, *Science* **271**, 1705 (1996).
  - <sup>47</sup>P. Sautet and C. Joachim, *Chem. Phys. Lett.* **153**, 511 (1998).
  - <sup>48</sup>C. Joachim and J. F. Vinuesa, *Europhys. Lett.* **33**, 635 (1996).
  - <sup>49</sup>M. Magoga and C. Joachim, *Phys. Rev. B* **56**, 4722 (1997).
  - <sup>50</sup>S. N. Yaliraki and M. A. Ratner, *J. Chem. Phys.* **109**, 5036 (1998).
  - <sup>51</sup>M. Di Ventra, S. T. Pantelides, and N. D. Lang, *Phys. Rev. Lett.* **84**, 979 (2000).
  - <sup>52</sup>J. Reichert, R. Ochs, D. Beckmann, H. B. Weber, M. Mayor, and H. v. Lhneysen, *Phys. Rev. Lett.* **88**, 176804 (2002).
  - <sup>53</sup>Y. Xue and M. A. Ratner, *Phys. Rev. B* **68**, 115406 (2003).
  - <sup>54</sup>Y. Xue and M. A. Ratner, *Phys. Rev. B* **69**, 085403 (2004).
  - <sup>55</sup>J. Taylor, M. Brandbyge, and K. Stokbro, *Phys. Rev. Lett.* **89**, 138301 (2002).
  - <sup>56</sup>R. Hofmann, *J. Chem. Phys.* **39**, 1397 (1963).